

MOL #40931

**Derlin-1 and p97/VCP Mediate the ER-Associated Degradation of Human V2
Vasopressin Receptors***

Isabel Schwieger, Katja Lautz, Eberhard Krause, Walter Rosenthal, Burkhard Wiesner and Ricardo
Hermosilla
Charité-Universitätsmedizin Berlin, Abteilung für Molekulare Pharmakologie und Zellbiologie,
Thielallee 71, 14195 Berlin, Germany (I.S., K.L., W.R., R.H.[†])

Running Title

Degradation of V2 vasopressin receptors

Corresponding Author

Ricardo Hermosilla, Leibniz-Institut für Molekulare Pharmakologie (FMP), Campus Buch, Robert-Rössle Str. 10, 13125 Berlin, Germany. Tel.+49-30-94793 257, FAX. +49-30-94793109, E-mail: ricardo.hermosilla@charite.de

| | |
|-------------------------------------|------|
| <u>No. of text pages</u> | 32 |
| <u>No. of tables</u> | 1 |
| <u>No. of figures</u> | 9 |
| <u>No. of references</u> | 38 |
| <u>No. of words in Abstract</u> | 234 |
| <u>No. of words in Introduction</u> | 694 |
| <u>No. of words in Discussion</u> | 1430 |

Abbreviations: AVP, 8-arginine vasopressin; BP, band pass; B_{MAX} , maximal binding; CP, core particle; DMEM, Dulbecco's modified Eagle's medium; EC_{50} , concentration at which 50% of the maximal effect is obtained; ECL, enhanced chemiluminescence; *EndoH*, endoglycosydase H; ER, endoplasmic reticulum; ERAD, ER-associated degradation; ERGIC, ER/Golgi intermediate compartment; FBS, fetal bovine serum; GFP, green fluorescent protein; HEK, human embryonic kidney; IgG, immunoglobulin class G; K_D , dissociation constant; NDI, nephrogenic diabetes insipidus; p97/VCP, valosin-containing protein; *PNGaseF*, peptide endoglycosydase F; RP, regulatory particle; Rpn1/S2, proteasome 26S non-ATPase subunit 2; Rpn10/S5a, 26S protease regulatory subunit 5a; Rpt1/S7, 26S protease regulatory subunit 7; UPR, unfolded protein response; V2R, human V2 vasopressin receptor.

MOL #40931

Abstract

The ER-associated degradation (ERAD), the main quality control pathway of the cell, is crucial for the elimination of unfolded or misfolded proteins. Several diseases are associated with the retention of misfolded proteins in the early secretory pathway. Among them is X-linked nephrogenic diabetes insipidus, caused by mutations in the gene encoding the V2 vasopressin receptor (V2R). We studied the degradation pathways of three intracellularly retained V2R mutants with different misfolded domains in HEK293 cells. At steady state, the wild type V2R and the complex-glycosylated mutant G201D were partially located in lysosomes, while core-glycosylated mutants L62P and V226E were excluded from this compartment. In pulse-chase experiments, proteasomal inhibition stabilized the non- and core-glycosylated forms of all studied receptors. In addition, all mutants and the wild type receptor were found to be polyubiquitinated. Non- and core-glycosylated receptor forms were located in cytosolic and membrane fractions, respectively, confirming the deglycosylation and retrotranslocation of ERAD substrates to the cytosol. Recently, distinct Derlin-1-dependent and -independent ERAD pathways have been proposed for proteins with different misfolded domains (cytosolic, extracellular and membrane) in yeast. Here we show for the first time that V2R mutants with different misfolded domains are able to co-precipitate the ERAD components p97/valosin-containing protein, Derlin-1 and the 26S proteasome regulatory subunit 7. Our results demonstrate the presence of a Derlin-1 mediated ERAD pathway degrading wild type and disease-causing V2R mutants with different misfolded domains in a mammalian system.

Introduction

Several human diseases are caused by the retention and/or accumulation of a protein within the cell. The quality control system of the secretory pathway screens for non-native protein conformations, e.g. unfolded or misfolded proteins, impedes their further transport and targets them to the degradation system. These proteins do not reach their site of action which leads to a loss of function and thereby to disease (Aridor and Hannan, 2000; Aridor and Hannan, 2002). Generally there are two fates for these retained proteins, either they are degraded or they accumulate. Protein accumulation in the endoplasmic reticulum (ER) may lead to an unfolded protein response (UPR) and/or ER overload response (Zhang and Kaufman, 2006). Other proteins may accumulate in the cytosol, which eventually leads to the formation of intracellular aggregates or aggresomes (Kopito, 2000), but ultimately in both cases, the cell is damaged and apoptosis is induced.

The intracellular retention of the V2 vasopressin receptor (V2R) causes X-linked nephrogenic diabetes insipidus (NDI). More than 170 different mutations of the *AVPR2* gene, each one of them causing NDI, have been described in the literature (<http://www.medicine.mcgill.ca/nephros>). The V2R is normally expressed at the plasma membrane of renal epithelial cells of the collecting duct and regulates vasopressin (AVP) mediated water reabsorption in the kidney. The majority of NDI-causing mutations produce receptors that are retained in different intracellular compartments, like the ER, ER/Golgi intermediate compartment (ERGIC) (Hermosilla et al., 2004) and Golgi apparatus. Few NDI-causing mutants are expressed at the cell surface, but fail to get activated by AVP (Robben et al., 2006). Patients with NDI suffer from polyuria, polydipsia, nocturia, and failure to thrive.

Disease-causing V2R mutants that are retained in different compartments of the secretory pathway are a good model to elucidate the interactions between the quality control system and degradation pathways. Intracellular degradation of membrane proteins is carried out by the lysosomes and/or the ubiquitin/proteasome system, depending on the intracellular localization of the protein. Proteins localized at the plasma membrane are usually degraded in lysosomes, such as the wild type V2R (Bouley et al., 2005). ER-retained proteins are targeted to the ER-associated degradation (ERAD) pathway. ER-retained misfolded membrane proteins are polyubiquitinated by ubiquitin ligases (gp78, Hrd1) and pulled out of the ER membrane by AAA-ATPases (p97/valosin-containing protein

MOL #40931

(p97/VCP)) and ATPases of the 19S proteasome (Meusser et al., 2005; Wahlman et al., 2007) through channel proteins, like Sec61 α and/or Derlin-1, -2 or -3. They are de-glycosylated, de-ubiquitinated and unfolded before being degraded by the 26S proteasome (Hampton, 2002; Werner et al., 1996). G protein-coupled receptors (GPCR), as the δ opioid receptor, luteinizing hormone receptor and some disease-causing V2R mutants, have been associated with proteasomal degradation in mammalian cells (Petäjä-Repo et al., 2001; Pietila et al., 2005; Robben et al., 2005), however their degradation mechanisms are not fully understood. Furthermore, it is unknown how receptor proteins are degraded that are neither retained in the ER, nor localized at the cell membrane, like V2R mutants that are retained in the ERGIC (V226E) and Golgi apparatus (G201D).

In yeast, three distinct ERAD pathways (ERAD-L for misfolded ER-luminal domains; -M, for misfolded intramembrane domains; -C, for misfolded cytosolic domains of substrate proteins) have been proposed (Carvalho et al., 2006). ERAD-L and -M require the ubiquitin ligase Hrd1 and its cofactor Hrd3, but not Doa10 as the ERAD-C pathway. Der1 (Derlin-1, -2, -3 in mammals) is required in the ERAD-L pathway. All ERAD pathways require the ATPase complex of Ubx2, Npl4, Ufd1, and Cdc48 (p97/VCP in mammals). So far, it is unknown whether these distinct pathways also operate in mammalian cells. In the present work, we analyzed the degradation pathways of the wild type V2R and of three NDI-causing V2R mutants with misfolded cytosolic (L62P), luminal (G201D) and intramembrane (V226E) domains that are retained in different intracellular compartments, namely the ER, ERGIC and Golgi apparatus, respectively. The wild type receptor and all intracellular retained mutants are polyubiquitinated and interact with the ERAD components Derlin-1, the AAA-ATPase p97/VCP, and the 26S proteasome regulatory subunit 7 (Rpt1/S7), regardless of the location of their misfolded domains. Our results show that substrates with different misfolded domains are degraded by a Derlin-1, p97/VCP-mediated ERAD pathway in HEK923 cells.

Materials and Methods

Materials. [^3H]cAMP (0.925 TBq/mmol), [α - ^{32}P] ATP (29.6 TBq/mmol) and [^{35}S] Easy tag protein labeling mix (43.48 TBq/mmol) were obtained from Perkin Elmer (Boston, USA). LipofectAMINETM 2000 was purchased from Invitrogen (Karlsruhe, Germany) and FuGENE 6 from ROCHE Diagnostics-Applied Science (Mannheim, Germany). Restriction enzymes were from New England Biolabs (Schwalbach, Germany). Trypsin (sequencing grade) was obtained from Promega (Madison, USA). PMSF, deoxycholic acid sodium salt, Roti-Load 1 and SDS were from Roth (Karlsruhe, Germany). Dulbecco's modified Eagle's medium (without methionine and cysteine), benzamidine, chloroquine diphosphate salt, protein A-Sepharose, protein G-Agarose, the rabbit polyclonal α -Derlin-1 antibody, mouse monoclonal α -actin antibody, rabbit polyclonal α -FLAG antibody, mouse monoclonal α -FLAG M2 antibody and α -FLAG M2 Affinity Gel were from Sigma (Munich, Germany). Aprotinin (Trasylol), Tween-20, Trypsin inhibitor (STI), and the Chemiluminescence detection kit for horseradish peroxidase (POD) were from AppliChem (Darmstadt, Germany). The POD-conjugated goat α -rabbit and goat α -mouse antibodies were purchased from Dianova (Hamburg, Germany). The rabbit α -p97/VCP antibody and the monoclonal rabbit α -GAPDH antibody were from Cell Signaling (Danvers, Ma, USA). The rabbit α -19S proteasome subunit Rpt1 antibody was from Biomol (Hamburg, Germany). The rabbit α -calnexin antibody and the monoclonal mouse anti-multi ubiquitin antibody were from Stressgen Bioreagents (Victoria, Canada). The polyclonal goat α -Derlin-1 antibody was from Santa Cruz Biotechnology (Santa Cruz, USA). LysoTracker[®] Red was from Molecular Probes (Eugene, Oregon, USA). MG 132 was purchased from Calbiochem (Darmstadt, Germany). Plasmid pV2R.DNA3.1, coding for the untagged V2R, and plasmid pEU367.GFP, encoding a C-terminally GFP-tagged V2R, have been described before (Oksche et al., 1998; Schülein et al., 1998). The pEGFP-N1 vector was from Clontech Laboratories (Heidelberg, Germany). The QuikChange[®] site-directed mutagenesis kit was purchased from Stratagene (La Jolla, USA) and the Qproteome cell compartment kit was from Qiagen (Hilden, Germany). HEK293 cells were purchased from DSMZ (Hannover, Germany).

MOL #40931

Plasmid constructions. Plasmid pFLAG.V2R encoding the V2R with a FLAG tag fused to the N terminus was made *via* PCR with a *Bam*HI /FLAG insertion primer (CGGGATCCCGGCCACCATGGA-CTATAAGGACGATGACGATAAGATGCTCATGGCGTCCACTTCCGC) and the commercially available pcDNA3.1/BGH reverse sequencing primer from Invitrogen. For this reaction, pV2R.DNA3.1 was used as a template. The PCR product, containing the FLAG.V2R cDNA and a N-terminally inserted *Bam*HI site, was cloned into the pcDNA3.1 vector using the introduced *Bam*HI site and an *Xba*I site. Plasmids pFLAG.L62P, pFLAG.V226E and pFLAG.G201D were constructed with the help of the QuikChange[®] site-directed mutagenesis kit (Stratagene; primer sequences available on request); plasmid pFLAG.V2R was used as template. Plasmids pL62P.GFP, pV226E.GFP and pG201D.GFP encoding the receptor mutants L62P, V226E and G201D tagged with GFP at their C terminus (residue K367) have been described elsewhere (Krause et al., 2000). Standard DNA preparations and cloning techniques were carried out according to the handbooks of Sambrook et al. (Sambrook and Russell, 2001). The nucleotide sequences of the DNA fragments were verified by sequencing, using the BigDye[®] Terminator kit (Applied Biosystems).

Cell culture. HEK293 cells were maintained in Dulbecco's modified Eagle's medium (DMEM) from Sigma, supplemented with 10% (v/v) heat-inactivated FBS, 20 mM glutamine, 100 IU of penicillin and 100 µg/ml streptomycin in a 5% CO₂ atmosphere at 37 °C. Stably expressing cell lines were generated through transfection with FuGENE 6 (Roche) or LipofectAMINE[™] 2000 (Invitrogen) according to the manufacturer's recommendations. Clones were selected with 400 µg/ml G418. The culture medium for the stably expressing cell clones was additionally supplemented with 400 µg/ml G418.

Adenylyl cyclase assay. The adenylyl cyclase assays were carried out with nuclei-free crude membranes of stably transfected HEK293 cells as described previously for stably transfected mouse Ltk⁻ cells (Schülelein et al., 1996).

MOL #40931

Total cell lysis. HEK293 cells stably expressing V2R constructs were grown to confluence on a 60 mm culture dish. Cells were washed two times with ice-cold PBS and lysed in 500 μ l Ripa buffer, the method has been described elsewhere (Gazit et al., 1999). After determination of protein concentration, 30 μ g of the total amount of proteins were used for SDS-PAGE.

Immunoprecipitation of FLAG-tagged V2Rs and co-immunoprecipitation. HEK293 cells stably expressing V2R constructs were grown to confluence on a 60 mm culture dish. Cells were washed two times with ice-cold PBS and lysed in 1 ml of ice-cold lysis buffer (1% Triton[®] X-100, 0.1% SDS, 50 mM Tris-HCl, 150 mM NaCl, 1 mM Na-EDTA, 0.5 mM PMSF, 10 μ g/ml STI, 1 μ g/ml Trasylol and 0.5 mM benzamidine, pH 8.0) and transferred to microfuge tubes. The insoluble fraction of one 60 mm culture dish was removed by centrifugation (20 min, 4 °C, 18,620 x g) and FLAG-tagged proteins were isolated from the supernatant with an immune complex of 5 mg protein A-Sepharose beads and 5 μ g α -FLAG Sigma M2 antibodies at 4 °C overnight. Beads were centrifuged (1 min, 4 °C, 13,680 x g), washed three times with buffer A (0.5% Triton[®] X-100, 0.1% SDS, 50 mM Tris-HCl, 500 mM NaCl, 1 mM Na-EDTA, pH 8.0) and once with buffer B (0.5% Triton[®] X-100, 0.1% SDS, 50 mM Tris-HCl, 1 mM Na-EDTA, pH 7.4). Bound proteins were eluted by 5 min boiling (95 °C) in 40 μ l of 2x Roti-Load 1 sample buffer and separated by SDS-PAGE. For co-immunoprecipitation experiments, FLAG-tagged proteins were isolated with 40 μ l of α -FLAG M2 Affinity Gel (Sigma) (same preparation as described above) or with an immune complex of 5 mg protein G-Agarose beads and 2 μ g of polyclonal α -Derlin-1 antibodies (Santa Cruz) at 4 °C overnight.

Immunoblots. Proteins were separated by SDS-PAGE (10% or 15% acrylamide) and blotted onto nitrocellulose membranes as described elsewhere (Kyhse-Andersen, 1984). Membranes were blocked for 1 h with PBS (140 mM NaCl, 2.7 mM KCl, 10 mM KH₂PO₄, pH 7.4) supplemented with 0.1% Tween-20 and 5% low fat milk powder and, in case of detection of the V2R, incubated with a mouse monoclonal α -FLAG M2 antibody (1:1500 in PBS with 0.1% Tween-20 and 2% low fat milk powder) for 1 h at RT. Membranes were washed three times (15 min each) with wash buffer (PBS supplemented with 0.1% Tween-20). Blots were incubated with a POD-conjugated α -mouse antibody

MOL #40931

(1:10,000) in PBS supplemented with 0.1% Tween-20 and 2% low fat milk powder for 45 min at RT. Membranes were washed again three times with wash buffer (15 min each). Finally, membranes were incubated in ECL for three minutes and developed with a luminescence X-Omat film (Kodak). For co-immunoprecipitation experiments a polyclonal α -p97/VCP antibody (Cell Signaling), a polyclonal rabbit α -Derlin-1 (Sigma), a polyclonal α -19S Regulator, ATPase subunit Rpt1 antibody (Biomol) (all at 1:1000 dilution) or a mouse monoclonal α -FLAG M2 antibody (Sigma) (1:1500 dilution) were used.

Ubiquitinylation assay. Stably transfected HEK293 cells were treated with 20 μ M MG 132 in serum-free medium for 16 h. Lysis of cells expressing FLAG-tagged receptors was carried out, the insoluble fraction was removed by centrifugation (20 min, 4 $^{\circ}$ C, 18,620 \times g) and polyubiquitinated proteins were isolated, as described in immunoprecipitation of FLAG-tagged V2Rs with 40 μ l of α -FLAG M2 Affinity Gel (Sigma). After the washing steps, the proteins were boiled in 40 μ l 2x Roti-Load 1 sample buffer, separated by SDS-PAGE (10% acrylamide) and blotted onto nitrocellulose membranes. For detection, a mouse monoclonal anti-multi ubiquitin antibody (Stressgen) (1:400) and a POD-conjugated α -mouse IgG (1:10,000) were used. The receptor expression was analyzed with a mouse monoclonal α -FLAG M2 antibody (Sigma) (1:1500) and a POD-conjugated α -mouse IgG (1:10,000). Immunoreactive bands were developed with ECL.

Visualization of GFP-tagged receptors by confocal laser-scanning microscopy in living HEK293 cells. Stably transfected HEK293 expressing the wild type and mutant V2Rs tagged with GFP were grown for 24 - 48 h in a 35 mm culture dish containing a poly-L-lysine-coated cover slip. Cells were incubated with 150 nM LysoTracker[®] for 1 h and for inhibition of degradation additionally incubated with 100 μ M chloroquine for 3 h, washed once with PBS and transferred immediately into a heating chamber (details on request). Cells were covered with 1 ml PBS and GFP fluorescence was visualized on a Zeiss 510 invert laser-scanning microscope (optical section: <0.9 μ m; λ_{exc} : 488 nm, LP filter: 505 nm). GFP and LysoTracker[®] fluorescence signals were recorded (optical section: <0.9 μ m; multitrack

MOL #40931

mode; GFP, λ_{exc} : 488 nm, BP filter: 494–548 nm; LysoTracker[®] Red, λ_{exc} : 543 nm, LP filter: 560 nm) and an overlay of both signals was computed.

Pulse-chase assay. Stably transfected HEK293 cells were grown in 100 mm culture dishes until confluence. Cells were starved in 5 ml serum-free DMEM without methionine and cysteine (Sigma) for 16 h. The cells were washed twice with PBS, treated with trypsin/EDTA, and collected in a 15 ml Falcon[®] tube. Cells were washed with PBS two more times (1,000 x g, RT, 5 min). Metabolic labeling with 220 μCi of [³⁵S] Easy tag protein labeling mix in 500 μl medium lacking methionine and cysteine was performed for 45 min. The labeling process was stopped with 4 ml DMEM supplemented with unlabeled methionine (2.3 mM) and cysteine (0.75 mM). To indicated times cells were resuspended and 1 ml suspension was harvested for each sample, mixed with 750 μl ice-cold DMEM supplemented with protease inhibitors (0.5 mM PMSF, 10 $\mu\text{g/ml}$ STI (trypsin inhibitor), 1 $\mu\text{g/ml}$ Trasylol and 0.5 mM benzamidine), collected by a centrifugation step (1,000 x g, 4 °C, 5 min) and lysed with 500 μl ice-cold lysis buffer. The FLAG-tagged receptors were immunoprecipitated as described above. After separation by SDS-PAGE (10% acrylamide), the gels were dried and exposed to X-ray film. Lysosomal and proteasomal activity was inhibited with 100 μM chloroquine and 40 μM MG 132, respectively, supplemented in all buffers from the labeling step until the end of the chase.

Protein identification by mass spectrometry. Proteins of HEK293 cells treated with and without MG 132 were immunoprecipitated, prepared as described above, and subjected to SDS-PAGE. Sample preparation, in-gel digestion, peptide extraction, and spectra acquisition were performed as described elsewhere (Czupalla et al., 2006). In brief, proteins were stained with Coomassie blue, excised from the gel and subjected to in-gel digestion by trypsin. NanoLC-MS/MS experiments were performed on a quadruple orthogonal acceleration time-of-flight mass spectrometer Q-ToF Ultima[™] (Micromass, Manchester, UK). A Micromass CapLC liquid-chromatography system with a capillary column (PepMap C₁₈, 3 μm , 150 mm x 75 μm i.d., Dionex, Idstein, Germany) was used to deliver the peptide solution to the nanoelectrospray source (PicoTip spray capillaries, New Objective, Woburn, MA, USA). For protein identification, data were acquired in a data-dependent mode (survey scanning)

MOL #40931

using one MS scan followed by MS/MS scans of the most abundant peak. The processed MS/MS spectra and MASCOT server version 1.9 (Matrix Science Ltd, London, UK) were used to search in-house against the SwissProt protein database (210906, 234112 sequences).

Subcellular fractionation. Proteins of different cellular compartments were obtained with the Qproteome cell compartment kit (Qiagen, Germany). Cytosolic and membrane fractions were isolated according to the manufacturer's protocol. Equal amounts of proteins were used for SDS-PAGE. The purity of the fractions was controlled by detection of calnexin and GAPDH, concurrently the proteins served as a loading control. Detection of receptor proteins was carried out with a monoclonal α -FLAG M2 antibody (Sigma) and a POD-conjugated α -mouse IgG. Immunoreactive bands were developed with the ECL system.

Results

Lysosomal degradation of V2 vasopressin receptors

The degradation of intracellularly retained GPCRs has not been characterized in detail. The subject of the present study was the degradation pathway of three intracellularly retained V2R mutants, with misfolded domains located in different parts of the receptor. The L62P mutation is localized in the first intracellular domain at the interface to the first transmembrane domain; G201D lays in the second extracellular loop and V226E in the fifth transmembrane domain (Fig. 1 A). Mutants L62P and V226E are deficient in their ability to stimulate the adenylyl cyclase; mutant G201D is partially deficient, thereby confirming their disease-causing nature (Fig. 1 B). All mutants also show a different subcellular localization. The L62P mutant is found exclusively in the ER, the V226E mutant in the ER and ERGIC and the G201D mutant localizes in the ER, ERGIC, Golgi apparatus and partially at the plasma membrane (Hermosilla et al., 2004) (see Fig. 2 and supp. Fig. 2). We first determined whether lysosomes are involved in the degradation of all mutants. To this end, the presence of the mutants in lysosomes was assessed in living HEK293 cells by confocal laser scanning microscopy. Cell clones stably expressing the V2R mutants tagged with the green fluorescent protein (GFP) were stained with

MOL #40931

the fluorescent lysosome marker LysoTracker[®]. GFP fluorescence signals were recorded on the green and the LysoTracker[®] signals on the red channel; overlays were computed. L62P and V226E were diffusely localized within the cell, excluding the nucleus (Fig. 2, *left panels*). LysoTracker[®] signals were detected as intracellular vesicles, frequently nearby the nucleus (Fig. 2, *middle panels*) and no co-localization with GFP signals could be identified in overlays of mutants L62P and V226E (Fig. 2, *right panels*). Mutant G201D was detected in vesicular structures and at the plasma membrane. Colocalization with LysoTracker[®] signals was observed (Fig. 2, *right panel*). GFP fluorescence signals from the wild type V2R were localized predominantly at the plasma membrane and in vesicular structures, which also colocalized with LysoTracker[®] signals.

To confirm these results, we inhibited lysosomal enzymes, which should lead to an increase in the co-localization between GFP fluorescence and LysoTracker[®] signals. Stably transfected HEK293 cells were treated with 100 μ M chloroquine for 3 h. Only in the case of mutant G201D and the wild type receptor GFP fluorescence signals were increased (Fig. 3, *left and right panels*). No change in the GFP fluorescence signals and colocalization status with lysosomes of mutant L62P and V226E could be observed. These results demonstrate that G201D and the wild type V2R, which reach the Golgi apparatus and plasma membrane, are transported to the lysosomal compartment for degradation at steady state. In contrast, mutants L62P and V226E retained by the quality control system in the ER or ER/ERGIC are excluded from lysosomal degradation.

MG 132 inhibits the degradation of immature forms of all mutants and the wild type V2R

Mutants L62P and V226E were excluded from lysosomal degradation by their retention in the ER and ERGIC. Hence, their degradation should be carried out by the proteasome. Therefore, we studied the proteasomal and lysosomal degradation of all mutants and wild type V2R in HEK293 cells stably expressing N-terminally FLAG-tagged V2R constructs (see Supplemental Data and supp. Fig. 1 for the pharmacological characterization). Pulse-chase metabolic labeling experiments were done in the presence of the lysosomal enzyme inhibitor chloroquine, the proteasomal inhibitor MG 132 and under control conditions (untreated). Immunoprecipitated proteins were identified by autoradiography. At 0 h the wild type V2R showed one prominent band at 38 and another at 35 kDa, the first corresponding

MOL #40931

to the core-glycosylated (*EndoH* and *PNGaseF* sensitive) and the second to the non-glycosylated receptor form (*EndoH* and *PNGaseF* resistant; see supp. Fig. 3) (Fig. 4, *left panel*). Both bands were present at 2.5 h of chase, additionally a third broader band running between 55 and 45 kDa appeared. This band corresponds to the mature, complex-glycosylated form of the receptor (see supp. Fig. 3). After 5 h and 10 h of chase the 35-kDa band became undetectable and only bands corresponding to the glycosylated receptor forms were present.

A similar band pattern was detected for mutant G201D. However, bands representing the complex-glycosylated receptor forms were less prominent. In contrast to the wild type V2R and mutant G201D, mutants V226E and L62P showed two bands only, corresponding to immature forms of the receptor (non- and core-glycosylated); complex-glycosylated forms were not detectable (Fig. 4, *left panel* and supp. Fig. 3). Under control conditions, the immature forms of mutants L62P and V226E persisted longer than that of mutant G201D and the wild type receptor, indicating that the forward transport of the latter is also responsible for a signal reduction (Fig. 4, *left panel*).

Treatment with 100 μ M chloroquine had no apparent effect on the band pattern of the wild type V2R, indicating that its lysosomal degradation half-life is longer than 10 h. For mutant G201D a change was only observed in the case of the complex-glycosylated band, confirming that the mutant is degraded in lysosomes. Mutants V226E and L62P showed no change in their band pattern, demonstrating that they do not reach the lysosomal compartment.

Additionally, cell clones were treated with the proteasomal inhibitor MG 132 and bands representing the non-glycosylated and core-glycosylated receptors (immature receptor forms) could be stabilized in all samples (Fig. 4, *right panel*). This result shows that proteasomal activity is involved in receptor degradation of the immature receptor forms. Taken together, these results demonstrate that the complex-glycosylated receptors are subjected to lysosomal degradation whereas non- and core-glycosylated receptor proteins are degraded by the proteasome. Thus, the ERGIC seems to be the last compartment in the secretory pathway that excludes membrane proteins from lysosomal degradation.

Wild type V2R and NDI-causing mutants are polyubiquitinated

MOL #40931

Mature forms of the mutant G201D and wild type V2R were degraded in lysosomes. In contrast, the immature forms of the wild type and mutant V2Rs were stabilized when proteasomal activity was blocked, demonstrating a participation of the proteasome in their degradation. ERAD substrates are usually polyubiquitinated and retrotranslocated from the ER to the cytosol for proteasomal degradation. We investigated if the NDI-causing mutants and the wild type V2R are polyubiquitinated and degraded *via* the ERAD. FLAG-tagged receptors were precipitated with a α -FLAG M2 Affinity Gel and ubiquitinated receptor proteins were identified with a monoclonal α -polyubiquitin antibody. An immunoreactive smear starting at 250 kDa was only detected in samples that contained receptor constructs (Fig. 5 A). MG 132 treatment increased the intensity of this smear that ranged from 250 to 60 kDa due to ubiquitin chains of different length. The wild type V2R and intracellular retained mutants were polyubiquitinated, indicating that they are suitable substrates for ERAD.

Furthermore, the precipitation efficiency and expression levels of the V2R constructs used for the immunoprecipitations were analyzed by western blot. No major difference in the expression of FLAG-tagged constructs could be detected between cell clones subjected to immunoprecipitation (Fig. 5 B). As expected, for the V2R wild type and mutant G201D all three receptor forms, the non-glycosylated, core-glycosylated (immature), and complex-glycosylated form could be detected after MG 132 treatment (compare supp. Fig. 3 & Fig. 4, *right panel*). Mutants V226E and L62P showed only immature receptor forms. Bands with an apparent molecular mass of ~160 and 80 kDa are presumably multimers of immature receptor proteins (Fig. 5 B, (*)). The apparent smear detected between 200 and 80 kDa represents polyubiquitinated forms of the V2R.

Wild type V2R and NDI-causing mutants interact with ERAD components

If the immature wild type V2R and its mutants are degraded *via* the ERAD, canonical ERAD components that interact with polyubiquitinated proteins should be identified after precipitation of V2R from HEK293 cells. Stably transfected cells expressing the FLAG-tagged wild type V2R were treated with and without MG 132 overnight and receptors were immunoprecipitated and separated by SDS-PAGE. Corresponding slices from Coomassie-stained gels of MG 132-treated and untreated

MOL #40931

samples were excised (for details see supp. Fig. 4). Co-precipitated proteins were in-gel digested with trypsin and identified by NanoLC-tandem mass spectrometry. In samples of untreated cells only the V2R and Ig gamma-1 chain of precipitating antibodies were detected. In samples of MG 132-treated cells, several proteins related to cell stress and protein degradation were identified additionally: immunoglobulin heavy chain-binding protein (BiP/Grp78), the 26S proteasome regulatory subunit 7 (Rpt1/S7), the proteasome 26S non-ATPase subunit 2 (Rpn1/S2), elongation factor 1- α 1 (eEF1A-1), heat shock protein 90kDa α (HSP 90- α /HSP 86) and heat shock protein 90kDa β (HSP 90- β /HSP 84) (Table 1). Both identified proteasomal proteins are subunits of the 19S proteasome regulatory complex.

To verify the mass spectrometry results, we first studied the endogenous expression levels of Rpt1/S7 in whole cell lysates from stable cell clones. A specific immunoreactive band running at 48 kDa was identified in all lysates (Fig. 6, *upper panel*); no difference in the expression of Rpt1/S7 could be detected between cell clones. Next, blots of immunoprecipitated samples pretreated with or without MG 132 showed also a specific band with an apparent mass of 48 kDa, representing Rpt1/S7, and an unspecific band of 60 kDa. In untreated samples of mutant L62P, more Rpt1/S7 could be co-precipitated than in other samples (Fig. 6, *middle panel*, Rpt1/S7). As expected, a strong increase in the intensity of the specific immunoreactive band could be observed, when cells were treated with MG 132 (Fig. 6, *lower panel*, Rpt1/S7). As a control for V2R precipitation levels the same membranes were stripped and used for V2R detection (Fig. 6, V2R). In the presence of MG 132 immature V2R forms were increased, partially explaining the increased co-immunoprecipitation of Rpt1.

Another canonical ERAD component is p97/VCP, an AAA-ATPase involved in the extraction of misfolded proteins from the ER. It binds to polyubiquitinated ERAD substrates. Expression levels of p97/VCP were analyzed in whole cell lysates by immunoblotting and again no differences could be detected between cell clones (Fig. 7, *upper panel*, p97/VCP). Co-immunoprecipitation studies showed an immunoreactive band with an apparent size of 89 kDa in samples of whole cell lysates detected against p97/VCP. No specific signals were found in co-immunoprecipitated samples from untreated cell clones. The only exception was mutant L62P, where a specific band running at 89 kDa could be identified, indicating an interaction of this mutant with p97/VCP at steady state (Fig. 7, *middle panel*,

MOL #40931

p97/VCP). As expected, treatment with MG 132 increased the amount of co-precipitated *p97/VCP* significantly (Fig. 7, *lower panel, p97/VCP*). *V2R* precipitation levels were assayed in the same membranes used for the co-immunoprecipitation study (Fig. 7, *V2R*).

Similar experiments were also performed with an antibody against Derlin-1, a membrane protein that acts in concert with the *p97/VCP* to remove dislocation substrate proteins from the ER membrane. A single band with an apparent size of 22 kDa could be identified in samples of whole cell lysates, with no differences in the expression levels between cell clones (Fig. 8 A, *upper panel, Derlin-1*). In immunoprecipitated samples of untreated cells, an immunoreactive band of 22 kDa could be detected with a α -Derlin-1 antibody (data not shown). As expected, the intensity of this band increased, when cells were treated overnight with MG 132 (Fig. 8 A, *middle panel, Derlin-1*). *V2R* precipitation levels were verified in the same membranes used for the detection of Derlin-1 (Fig. 8 A, *lower panel, V2R*). Additionally, we also precipitated Derlin-1 and detected against the *V2R* with a mouse monoclonal α -FLAG M2 antibody. As expected, only immature forms of all mutants and the wild type *V2R* were co-precipitated by Derlin-1 in a MG 132-dependent manner (Fig. 8 B). Unfortunately, reverse co-immunoprecipitation studies were not successful using α -Rpt1 and α -*p97/VCP* antibodies for precipitation.

Proteasomal inhibition leads to an accumulation of immature, polyubiquitinated and non-polyubiquitinated proteins, thereby increasing the amount of immunoprecipitated receptors and co-precipitated proteins, in this case Rpt1/S7, *p97/VCP* and Derlin-1, confirming that these proteins bind polyubiquitinated ERAD substrates (Wang et al., 2004) (see Fig. 5 A & B, Fig. 6 – 8, *V2R*). Our results show that immature and/or polyubiquitinated *V2Rs* interact with ERAD components, namely Rpt1/S7, *p97/VCP* and Derlin-1. However, these results do not preclude the possibility that other ERAD proteins participate in this complex.

Immature receptor proteins are retrotranslocated into the cytosol

V2R mutants are polyubiquitinated and interact with membrane and cytosolic components of the ERAD complex. For determination of the site of turnover, cytosolic and membrane fractions of HEK293 cells stably expressing FLAG-tagged L62P mutants and wild type receptors were isolated.

MOL #40931

Immunoblot analysis revealed specific bands in the cytosolic and membrane fractions of MG 132-treated cells (Fig. 9). In the cytosolic fraction of L62P a specific band of approximately 35 kDa could be detected that corresponds to the un-glycosylated receptor form. In the membrane fraction a specific band of 38 kDa could be identified, representing the core-glycosylated receptor form. For the wild type receptor a similar band pattern could be recognized, however in the membrane fraction of MG 132-treated cells two additional immunoreactive bands could be detected, one between 53 - 45 kDa and a second of 35 kDa. These bands represent the complex- and un-glycosylated receptor forms, respectively. As expected, an increase in the intensity or emergence of bands representing the immature receptor forms was observed in cells treated with MG 132, confirming our results obtained by pulse-chase analysis. These results indicate that ERAD substrates are de-glycosylated and retrotranslocated completely into the cytosol. Furthermore, glycosylated receptor forms are restricted to the membrane fraction.

Taken together, our results demonstrate that core-glycosylated disease-causing mutants of the V2R are retrotranslocated, de-glycosylated and degraded *via* a Derlin-1 and p97/VCP mediated ERAD pathway. This degradation pathway is independent of the location of the misfolded domain within the V2R.

Discussion

Two major pathways may operate in the cell to degrade intracellularly retained GPCRs: the ubiquitin-dependent proteasomal and the lysosomal pathways (Ciechanover, 2006). It is accepted that integral membrane proteins expressed at the cell surface are internalized and degraded by the lysosome. On the other hand, membrane proteins retained in the ER by the quality control system are retrotranslocated into the cytosol and degraded by the ubiquitin/proteasome system. This particular degradation pathway is known as ERAD (Brodsky and McCracken, 1999; Hampton, 2002). In mammalian cells the ERAD pathway is still not well characterized. In addition, the degradation pathways utilized by the cell when proteins are retained outside the ER are also not well defined.

MOL #40931

In the present study, we analyzed the degradation pathways of the wild type V2R and three intracellularly retained disease-causing mutants. These particular mutants are good tools to analyze the degradation pathways, because they are retained in different compartments of the secretory pathway (Hermosilla et al., 2004). Furthermore, the defects resulting from mutations are localized in different domains of the protein; L62P is located in a cytosolic domain (beginning of the first intracellular loop), G201D in a luminal (second extracellular loop) and V226E in a transmembrane domain (fifth helix) (Fig. 1 A). The co-localization studies in living cells showed that the wild type V2R and mutant G201D are localized in lysosomes. Furthermore, pulse-chase experiments demonstrated that the complex glycosylated (mature) forms of mutant G201D are degraded by lysosomes. Similar results have been reported for the wild type V2R and mature mutants at steady state and after activation by AVP (Robben et al., 2004). Our results demonstrate that membrane proteins, which reach the Golgi apparatus or are expressed at the plasma membrane, are transported to the lysosomal compartment for degradation at steady state. However, it is not known whether receptors that reach the Golgi apparatus are first transported to the plasma membrane and then to lysosomes, or if a direct route is followed or if both routes are operating.

All immature V2R forms (mutant and wild type) were degraded *via* the ERAD, regardless of their intracellular localization (Fig. 6 – 8; supp. Fig. 2). As expected, all mutants were found out to be polyubiquitinated (Fig. 5 A & B). We could demonstrate that in the presence of a proteasome inhibitor all non- and core-glycosylated V2R proteins were stabilized (Fig. 4, *MG 132* & Fig. 5 B), and that wild type and mutant receptors co-precipitated Derlin-1, p97/VCP, Rpt1/S7 and Rpn2/S2. These results indicate that newly synthesized misfolded or unfolded receptors are targeted to the ERAD by the quality control system. Therefore, we conclude that the ERAD is predominantly involved in the degradation of immature disease-causing V2R mutants, but also of immature, misfolded wild type V2Rs. The fact that also immature wild type proteins are degraded by the ERAD has been described for the δ opioid (Petäjä-Repo et al., 2001), luteinizing hormone receptor (Pietila et al., 2005) and the cystic fibrosis transmembrane regulator (CFTR) and ascribed to inefficient folding or structural instability of the proteins (Sun et al., 2006). These data show that only non- and core-glycosylated misfolded receptor proteins are degraded *via* ERAD and that complex-glycosylated misfolded receptor

MOL #40931

proteins are targeted to lysosomal degradation. Our results demonstrate that the ERGIC is the last compartment of quality control that participates in ERAD.

The wild type V2R has been described to be ubiquitinated together with β -arrestin 2, but only after agonist induced internalization; both proteins are thought to be transported together to the lysosomal compartment for degradation (Martin et al., 2003). The ubiquitin ligases involved in the polyubiquitination of immature wild type V2Rs and NDI-causing mutants are still unknown. Most probable ubiquitin ligases like gp78/autocrine motility factor receptor (membrane-associated E3), Hrd1 (membrane-associated E3) and Ufd2 (E4 enzyme), that interact with p97/VCP and participate in the retrotranslocation of ERAD substrates (Ye, 2006), are involved in the polyubiquitination of immature forms of the V2R. In an attempt to determine the E3 that is responsible for the polyubiquitination of NDI-causing V2R mutants, immunoprecipitated samples were analyzed for the presence of Hrd1. It was not possible for us to detect specifically Hrd1 in these samples (data not shown).

In yeast, three distinct ERAD pathways have been proposed: the ERAD-L, -M and -C, which destroy proteins with misfolded luminal, intramembrane and cytosolic domains, respectively (Carvalho et al., 2006). These pathways use the cytosolic Cdc48 ATPase complex, whose membrane recruitment is facilitated by Ubx2. However, the ERAD-L and -M pathway require the ubiquitin ligase Hrd1, additionally ERAD-L needs Der1; both proteins have mammalian homologues (Hrd1, gp78 and Derlin-1, -2, -3) that are involved in the mammalian ERAD. ERAD-C requires the ubiquitin ligase Doa10, but not Hrd1 and Der1. Our results for the studied V2R mutants suggest that only the Derlin-1-mediated ERAD pathway is used in HEK293 cells. Regardless of their misfolded domain either cytosolic (L62P), luminal (G201D) or membrane (V226E), all mutants precipitated Derlin-1 and p97/VCP, the mammal homolog of Cdc48. We also investigated a second mutant with a mutation within the fourth transmembrane domain (S167L) that also interacts with Derlin-1 (data not shown). Our results demonstrate that at least the putative channel protein Derlin-1 and the AAA-ATPase p97/VCP are central components of the retrotranslocation machinery of the ERAD in a mammalian system.

MOL #40931

Sec61 α and Derlin-1 (and its homologs, Derlin-2 and -3) are thought to be the channel or to be located at the site of retrotranslocation of misfolded proteins from the ER to the cytosol (Kalies et al., 2005; Ye et al., 2005; Ye et al., 2004). It is still unclear whether the proteasome is recruited to the ER membrane by binding to the retrotranslocation channel, so that substrates are directly released into the proteasome (Kalies et al., 2005) or if substrates are first released into the cytosol and then targeted to the proteasome (Meusser et al., 2005; Petäjä-Repo et al., 2001). It has been shown that the 26S proteasome disassembles in an ATP-dependent catalytic cycle, leading to 19S RP subcomplexes and free Rpn10/S5a (Babbitt et al., 2005). On the other hand, 19S RPs are able to interact with Sec61 at the ER membrane (Ng et al., 2007). Recently, Wahlman et al. demonstrated that ATP, the 19S RP, the ER luminal chaperone PDI and Derlin-1 are sufficient to retrotranslocate a soluble ERAD substrate *in vitro* (Wahlman et al., 2007). Interestingly, retrotranslocation of the substrate was ubiquitin, Sec61 α , p97/VCP, and Ufd1 and Npl4 cofactors independent. However, the ERAD substrate used in this study was the fluorescence-labeled Δ gp α f, a soluble, non-ubiquitinated protein lacking disulfide bonds and transmembrane domains, which is derivative of the yeast pro- α factor mating pheromone. In our system, V2Rs were located in the ER-membrane, glycosylated, and/or polyubiquitinated, which might explain the differences regarding the association with p97/VCP. Furthermore, we could identify de-glycosylated V2R (wild type and mutant) in the cytosolic fraction after proteasomal inhibition, indicating a complete retrotranslocation of the receptors to the cytosol. Our results support the idea that 19S RP plays a central role in retrotranslocation and recognition of ERAD substrates, prior to their degradation by the 26S proteasome. Since retrotranslocated V2Rs seemed not to be polyubiquitinated, the interaction with 19S RP might induce their deubiquitination. Therefore, we propose that subunits of the 19S RP, like Rpt1/S7, Rpn1/S2 and Rpn10/S5a, function as scaffolds on the ER-substrate for the 19S RP and 20S CP, facilitating the assembly of the 26S proteasome at the substrate. Moreover, Derlin-1 is centrally implicated in the recognition and/or retrotranslocation of the V2R, independent of the location of the misfolded domain.

Until now, no effective pharmacological treatment of NDI has been developed. A promising therapeutic strategy is the use of pharmacochaperones that rescue transport defective receptors from the early secretory pathway to the plasma membrane (Bernier et al., 2006; Wüller et al., 2004).

MOL #40931

Another possible approach to rescue intracellularly retained proteins may be the inhibition of the ERAD, as exemplary shown for the CFTR by reducing the expression of p97/VCP or blocking the proteasome with bortezomib (Vij et al., 2006). However, this new therapeutic strategy may be only valid for NDI-causing mutants that are transport defective, but still functional.

In summary, our data reveal that the quality control system of the cell determines the degradation pathway of NDI-causing mutants of the V2R. Immature receptor proteins that reach the ERGIC are polyubiquitinated and degraded *via* the ERAD, all other mature receptor proteins located beyond the ERGIC are degraded *via* lysosomes. Furthermore, we demonstrate that a Derlin-1 and p97/VCP-mediated ERAD pathway is responsible for the degradation of the V2R and its disease-causing mutants, regardless of the location of the misfolded domain within the receptor.

Acknowledgements

We thank Ursula Brandt, Stefani Schneider and Michael Schümann for excellent technical work, Philipp Voigt for technical advice and Ralf Schüle, Márta Szaszák and Evelina Grantcharova for critical reading of the manuscript and helpful discussions.

REFERENCES

Aridor M and Hannan LA (2000) Traffic jam: a compendium of human diseases that affect intracellular transport processes. *Traffic* **1**:836-851.

Aridor M and Hannan LA (2002) Traffic jams II: an update of diseases of intracellular transport. *Traffic* **3**:781-790.

Babbitt SE, Kiss A, Deffenbaugh AE, Chang YH, Bailly E, Erdjument-Bromage H, Tempst P, Buranda T, Sklar LA, Baumler J, Gogol E and Skowyra D (2005) ATP hydrolysis-dependent disassembly of the 26S proteasome is part of the catalytic cycle. *Cell* **121**:553-565.

Bernier V, Morello JP, Zarruk A, Debrand N, Salahpour A, Lonergan M, Arthus MF, Laperrière A, Brouard R, Bouvier M and Bichet DG (2006) Pharmacologic chaperones as a potential treatment for X-linked nephrogenic diabetes insipidus. *J Am Soc Nephrol* **17**:232-243.

Bouley R, Lin HY, Raychowdhury MK, Marshansky V, Brown D and Ausiello DA (2005) Downregulation of the vasopressin type 2 receptor after vasopressin-induced internalization: involvement of a lysosomal degradation pathway. *Am J Physiol Cell Physiol* **288**:C1390-1401.

Brodsky JL and McCracken AA (1999) ER protein quality control and proteasome-mediated protein degradation. *Semin Cell Dev Biol* **10**:507-513.

Carvalho P, Goder V and Rapoport TA (2006) Distinct ubiquitin-ligase complexes define convergent pathways for the degradation of ER proteins. *Cell* **126**:361-373.

Ciechanover A (2006) Intracellular Protein Degradation: From a Vague Idea Thru the Lysosome and the Ubiquitin-Proteasome System and onto Human Diseases and Drug Targeting. *Exp Biol Med* **231**:1197-1211.

Czupalla C, Mansukoski H, Riedl T, Thiel D, Krause E and Hoflack B (2006) Proteomic analysis of lysosomal acid hydrolases secreted by osteoclasts: implications for lytic enzyme transport and bone metabolism. *Mol Cell Proteomics* **5**:134-143.

MOL #40931

Gazit G, Lu J and Lee AS (1999) De-regulation of GRP stress protein expression in human breast cancer cell lines. *Breast Cancer Res Treat* **54**:135-146.

Hampton RY (2002) ER-associated degradation in protein quality control and cellular regulation. *Curr Opin Cell Biol* **14**:476-482.

Hermosilla R, Oueslati M, Donalies U, Schönenberger E, Krause E, Oksche A, Rosenthal W and Schülein R (2004) Disease-causing V(2) vasopressin receptors are retained in different compartments of the early secretory pathway. *Traffic* **5**:993-1005.

Kalies KU, Allan S, Sergeyenko T, Kroger H and Romisch K (2005) The protein translocation channel binds proteasomes to the endoplasmic reticulum membrane. *EMBO J* **24**:2284-2293.

Kopito RR (2000) Aggresomes, inclusion bodies and protein aggregation. *Trends Cell Biol* **10**:524-530.

Krause G, Hermosilla R, Oksche A, Rutz C, Rosenthal W and Schülein R (2000) Molecular and conformational features of a transport-relevant domain in the C-terminal tail of the vasopressin V2 receptor. *Mol Pharmacol* **57**:232-242.

Kyhse-Andersen J (1984) Electrophoretic transfer of multiple gels: a simple apparatus without buffer tank for rapid transfer of proteins from polyacrylamide to nitrocellulose. *J Biochem Biophys Methods* **10**:203-209.

Martin NP, Lefkowitz RJ and Shenoy SK (2003) Regulation of V2 vasopressin receptor degradation by agonist-promoted ubiquitination. *J Biol Chem* **278**:45954-45959.

Meusser B, Hirsch C, Jarosch E and Sommer T (2005) ERAD: the long road to destruction. *Nat Cell Biol* **7**:766-772.

Ng W, Sergeyenko T, Zeng N, Brown JD and Romisch K (2007) Characterization of the proteasome interaction with the Sec61 channel in the endoplasmic reticulum. *J Cell Sci* **120**:682-691.

MOL #40931

Oksche A, Dehe M, Schülein R, Wiesner B and Rosenthal W (1998) Folding and cell surface expression of the vasopressin V2 receptor: requirement of the intracellular C-terminus. *FEBS Lett* **424**:57-62.

Petäjä-Repo UE, Hogue M, Laperrière A, Bhalla S, Walker P and Bouvier M (2001) Newly synthesized human delta opioid receptors retained in the endoplasmic reticulum are retrotranslocated to the cytosol, deglycosylated, ubiquitinated, and degraded by the proteasome. *J Biol Chem* **276**:4416-4423.

Pietila EM, Tuusa JT, Apaja PM, Aatsinki JT, Hakalahti AE, Rajaniemi HJ and Petäjä-Repo UE (2005) Inefficient Maturation of the Rat Luteinizing Hormone Receptor: A PUTATIVE WAY TO REGULATE RECEPTOR NUMBERS AT THE CELL SURFACE. *J Biol Chem* **280**:26622-26629.

Robben JH, Knoers NV and Deen PM (2004) Regulation of the vasopressin V2 receptor by vasopressin in polarized renal collecting duct cells. *Mol Biol Cell* **15**:5693-5699.

Robben JH, Knoers NV and Deen PM (2005) Characterization of vasopressin V2 receptor mutants in nephrogenic diabetes insipidus in a polarized cell model. *Am J Physiol Renal Physiol* **289**:F265-272.

Robben JH, Knoers NV and Deen PM (2006) Cell biological aspects of the vasopressin type-2 receptor and aquaporin 2 water channel in nephrogenic diabetes insipidus. *Am J Physiol Renal Physiol* **291**:F257-270.

Sambrook J and Russell DW (2001) *Molecular cloning: A laboratory manual*. Cold Spring Harbor Laboratory Press, Cold Spring Harbor, New York.

Schülein R, Hermosilla R, Oksche A, Dehe M, Wiesner B, Krause G and Rosenthal W (1998) A dileucine sequence and an upstream glutamate residue in the intracellular carboxyl terminus of the vasopressin V2 receptor are essential for cell surface transport in COS.M6 cells. *Mol Pharmacol* **54**:525-535.

MOL #40931

Schülein R, Liebenhoff U, Müller H, Birnbaumer M and Rosenthal W (1996) Properties of the human arginine vasopressin V2 receptor after site-directed mutagenesis of its putative palmitoylation site. *Biochemical J* **313** (Pt 2):611-616.

Sun F, Zhang R, Gong X, Geng X, Drain PF and Frizzell RA (2006) Derlin-1 promotes the efficient degradation of the cystic fibrosis transmembrane conductance regulator (CFTR) and CFTR folding mutants. *J Biol Chem* **281**:36856-36863.

Vij N, Fang S and Zeitlin PL (2006) Selective Inhibition of Endoplasmic Reticulum-associated Degradation Rescues Δ F508-Cystic Fibrosis Transmembrane Regulator and Suppresses Interleukin-8 Levels: THERAPEUTIC IMPLICATIONS. *J Biol Chem* **281**:17369-17378.

Wahlman J, Demartino GN, Skach WR, Bulleid NJ, Brodsky JL and Johnson AE (2007) Real-Time Fluorescence Detection of ERAD Substrate Retrotranslocation in a Mammalian In Vitro System. *Cell* **129**:943-955.

Wang Q, Song C and Li CC (2004) Molecular perspectives on p97-VCP: progress in understanding its structure and diverse biological functions. *J Struct Biol* **146**:44-57.

Werner ED, Brodsky JL and McCracken AA (1996) Proteasome-dependent endoplasmic reticulum-associated protein degradation: An unconventional route to a familiar fate. *Proc Natl Acad Sci USA* **93**:13797-13801.

Wüller S, Wiesner B, Löffler A, Furkert J, Krause G, Hermosilla R, Schaefer M, Schülein R, Rosenthal W and Oksche A (2004) Pharmacochaperones post-translationally enhance cell surface expression by increasing conformational stability of wild-type and mutant vasopressin V2 receptors. *J Biol Chem* **279**:47254-47263.

Ye Y (2006) Diverse functions with a common regulator: ubiquitin takes command of an AAA ATPase. *J Struct Biol* **156**:29-40.

MOL #40931

Ye Y, Shibata Y, Kikkert M, van Voorden S, Wiertz E and Rapoport TA (2005) Inaugural Article: Recruitment of the p97 ATPase and ubiquitin ligases to the site of retrotranslocation at the endoplasmic reticulum membrane. *Proc Natl Acad Sci USA* **102**:14132-14138.

Ye Y, Shibata Y, Yun C, Ron D and Rapoport TA (2004) A membrane protein complex mediates retro-translocation from the ER lumen into the cytosol. *Nature* **429**:841-847.

Zhang K and Kaufman RJ (2006) The unfolded protein response: a stress signaling pathway critical for health and disease. *Neurology* **66**:S102-109.

MOL #40931

FOOTNOTES

* This work was supported by the Deutsche Forschungsgemeinschaft (DFG) grant DFG HE4468 – 1/1
& 1/2.

† Reprint requests to:

Prof. Dr. Ricardo Hermosilla

Leibniz-Institut für Molekulare Pharmakologie (FMP)

Robert-Rössle Str. 10

13125 Berlin

Germany

E-mail: ricardo.hermosilla@charite.de

MOL #40931

LEGENDS FOR FIGURES

Fig. 1. *A*, two-dimensional model of the V2R and three NDI-causing mutants. The amino acid sequence of the receptor is shown in one letter code, N-glycosylation at position N22, disulfide bond between C112 and C192 and palmitoylation of residues C341 and C342 are depicted. Substituted amino acids of mutants L62P, V226E, and G201D are shown in black. *B*, adenylyl cyclase activity assay with crude membranes of stably transfected HEK293 cells expressing the FLAG-tagged wild type and mutant V2Rs. Crude membranes were stimulated with 100 nM AVP, controls were performed in the absence of AVP. Data represent mean values of three independent experiments each performed in triplicate. Triplicates differed by less than 10%. SEM are depicted.

Fig. 2. Lysosomal localization of GFP-tagged wild type V2R and mutants L62P, V226E, and G201D analyzed in stably expressing living HEK293 cells. Cells were incubated with 150 nM LysoTracker[®] for 1 h and were examined by confocal laser scanning microscopy with horizontal (*xy*) scans. Receptor GFP fluorescence signals are shown in green (left panels) and LysoTracker[®] staining of the same cells in red (central panels). GFP and LysoTracker[®] Red fluorescence signals were computer-overlaid (right panels; overlap is indicated by yellow). The scans show representative cells. Scale bar, 10 μ m. Similar data were obtained in five independent experiments.

Fig. 3. Inhibition of lysosomal degradation analyzed in living HEK293 cells stably expressing the GFP-tagged wild type V2R and mutants L62P, V226E, and G201D. Cells were incubated with 100 μ M chloroquine for 3 h and 150 nM LysoTracker[®] for 1 h and were examined by confocal laser scanning microscopy with horizontal (*xy*) scans. Receptor GFP fluorescence signals are shown in green (left panels) and LysoTracker[®] staining of the same cells in red (central panels). GFP and LysoTracker[®] Red fluorescence signals were computer-overlaid (right panels; overlap is indicated by yellow). The scans show representative cells. Scale bar, 10 μ m. Similar data were obtained in five independent experiments.

MOL #40931

Fig. 4. Degradation of wild type V2R and NDI-causing mutants in stably expressing HEK293 cells. Cells expressing the FLAG-tagged wild type V2R and receptor mutants L62P, V226E and G201D were starved in serum-free DMEM without methionine and cysteine for 16 h and metabolically labeled with 220 μ Ci [35 S] Easy tag protein labeling mix for 45 min without (left panel) or with 100 μ M chloroquine (center) or 40 μ M MG 132 (right panel). The metabolic labeling was stopped and at time points 0, 2.5, 5, and 10 h the cells were harvested, lysed and immunoprecipitated as described in experimental procedures and separated by SDS-PAGE. The gels were dried and exposed to X-ray film. Molecular mass markers are shown on the right. The results are representative of three independent experiments.

Fig. 5. Ubiquitinylation and immunoprecipitation of FLAG-tagged V2R receptor constructs. *A*, Immunoprecipitation of polyubiquitinated receptors. HEK293 cells stably expressing wild type and mutant V2Rs were treated with 20 μ M MG 132 for 16 h (+) or left untreated (-). Proteins eluted from α -FLAG M2 Affinity Gel were analyzed by SDS-PAGE and western blot analysis with a monoclonal mouse α -polyubiquitin antibody and a POD-conjugated α -mouse antibody. *B*, stably expressing HEK293 cells were lysed and receptors immunoprecipitated with a α -FLAG M2 Affinity Gel as in *A* and detected with a mouse monoclonal α -FLAG M2 antibody, a POD-conjugated α -mouse antibody and the ECL system. Control: untransfected HEK293 cells. (*) indicates presumed V2R multimers. Data are representative of six independent experiments.

Fig. 6. Total cell lysates analyzed for Rpt1/S7 expression by western blotting (top panel). HEK293 cells stably expressing wild type and mutant V2Rs were treated with 20 μ M MG 132 for 16 h (+) or left untreated (-). Immunoprecipitation of FLAG-tagged V2R wild type and mutant receptors was performed and analyzed by immunoblotting in the two middle panels. Detection of co-precipitated subunits of the 26S proteasome was done with a polyclonal rabbit α -Rpt1/S7 antibody and a POD-conjugated α -rabbit antibody. V2R precipitation levels of the stripped membrane used for Rpt1 detection in the presence of MG 132 are shown in the lower panel. Controls were non-transfected HEK293 cells. Data are representative of four independent experiments.

MOL #40931

Fig. 7. Interaction of the V2R and NDI-causing mutants with p97/VCP. HEK293 cells stably expressing wild type and mutant V2Rs were treated with 20 μ M MG 132 for 16 h (+) or left untreated (-). Total cell lysates analyzed for p97/VCP expression by western blotting are shown in the top panel. Immunoprecipitation of the V2R wild type and mutant receptors was carried out and analyzed by western blotting in the two middle panels. Detection of co-precipitated p97/VCP was done with a polyclonal rabbit α -p97/VCP antibody, POD-conjugated α -rabbit antibody, and the ECL system. V2R precipitation levels of the stripped membrane used for p97/VCP detection in the presence of MG 132 are shown in the lower panel. Controls were non-transfected HEK293 cells. Data are representative of four independent experiments.

Fig. 8. Interaction of the V2R and NDI-causing mutants with Derlin-1. *A*, HEK293 cells stably expressing wild type and mutant V2Rs were treated with 20 μ M MG 132 for 16 h (+) or left untreated (-). Total cell lysates of untreated cells analyzed for Derlin-1 expression by western blotting are shown in the top panel. Actin was used as loading control. Immunoprecipitation of the wild type V2R and mutant receptors was carried out as described in Experimental Procedures and analyzed by western blotting. Detection of co-precipitated Derlin-1 was done with a polyclonal rabbit α -Derlin-1 antibody, POD-conjugated α -rabbit antibody, and the ECL system. V2R precipitation levels of the stripped membrane used for Derlin-1 detection in the presence of MG 132 are shown in the lower panel. Controls were non-transfected HEK293 cells. *B*, Co-immunoprecipitation study of the interaction between Derlin-1 and the V2R and its disease-causing mutants. Precipitations were done with a polyclonal α -Derlin-1 antibody (Santa Cruz) and detection was performed with a monoclonal α -FLAG M2 antibody. Specific bands, representing the immature forms of the V2R, could only be detected in the presence of MG 132. Controls were non-transfected HEK293 cells. Data are representative of four independent experiments.

Fig. 9. Cellular fractions analyzed for V2R expression. Stably expressing HEK293 cells were either treated with 20 μ M MG 132 for 16 h (+) or left untreated (-). Isolated cytosolic (c) and membrane (m)

MOL #40931

fractions were analyzed by SDS-PAGE and immunoblotting. Detection of FLAG-tagged V2R constructs was done with a mouse monoclonal α -FLAG M2 antibody and a POD-conjugated α -mouse antibody. Controls were non-transfected HEK293 cells (control). The purity of cell fractions was confirmed by the detection of calnexin and GAPDH in all isolated fractions. Data are representative of three independent experiments.

MOL #40931

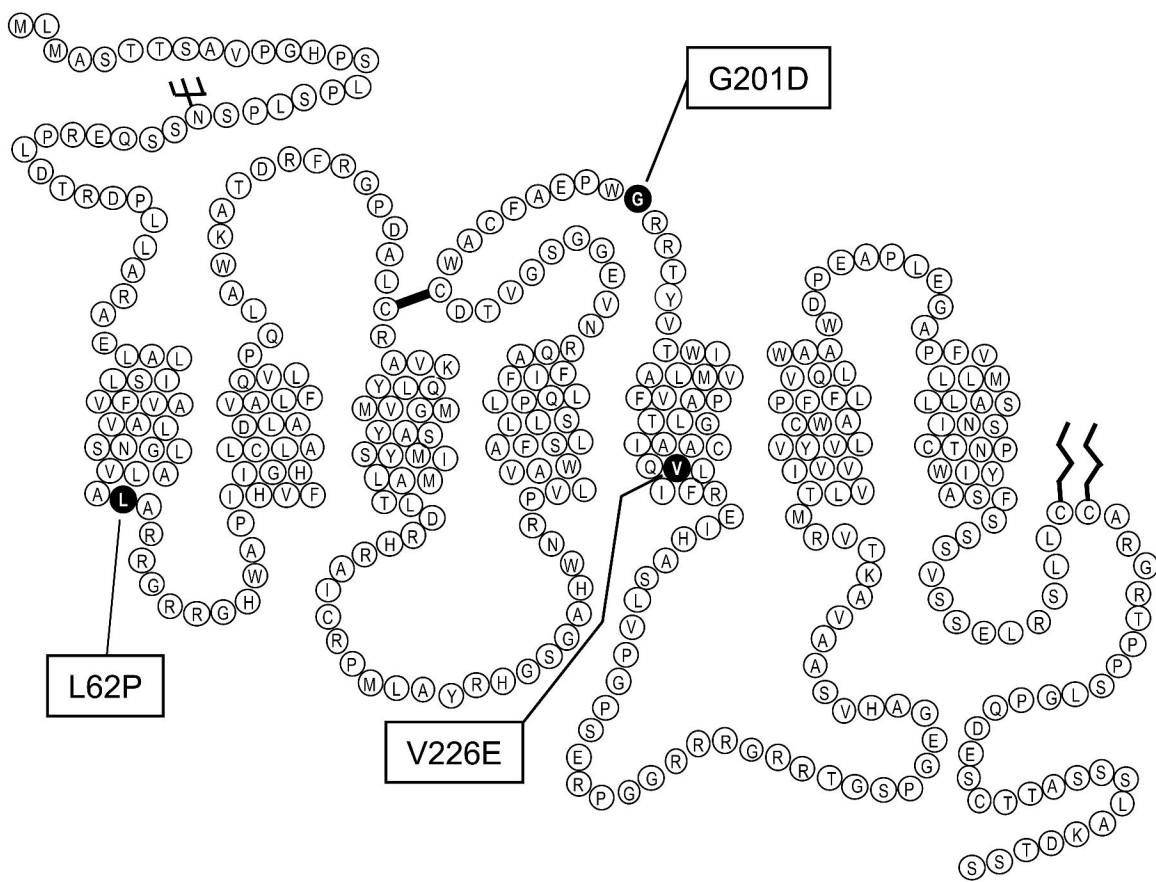
Table 1. V2R-associated proteins identified by NanoLC-ESI-MS/MS in the presence of MG 132

| Protein | SwissProt | Molecular mass <i>Da</i> | Score | Peptides (MS/MS) |
|--|-----------|-----------------------------|-------|---------------------|
| Immunoglobulin heavy chain-binding protein (GRP78/BiP) | P11021 | 72288 | 1399 | 23 |
| 26S proteasome ATPase regulatory subunit 7 (Rpt1/S7) | P35998 | 48472 | 352 | 5 |
| 26S proteasome non-ATPase regulatory subunit 2 (Rpn1/S2) | Q13200 | 100136 | 447 | 9 |
| Elongation factor 1-a1 (eEF1A-1) | P68104 | 50109 | 621 | 13 |
| Heat shock protein HSP 90- β (HSP 84) | P08238 | 83081 | 390 | 8 |
| Heat shock protein HSP 90- α (HSP 86) | P07900 | 84476 | 253 | 5 |
| Human V2 vasopressin receptor (V2R) | P30518 | 40253 | 246 | 5 |
| Mouse Ig gamma-1 chain C region (IgG1) | P01869 | 43359 | 206 | 4 |

Table 1. V2R-associated proteins identified by NanoLC-MS/MS. V2Rs expressed in the presence of MG 132 were immunoprecipitated *via* their FLAG tag and separated by SDS-PAGE. Co-precipitated proteins were stained with Coomassie blue, excised from the gel and subjected to in-gel digestion by trypsin. NanoLC-MS/MS experiments were performed and peptides identified in a data-dependent mode (survey scanning) using one MS scan followed by MS/MS scans of the most abundant peak. The most abundant proteins identified are shown. Proteins listed were not found in cells that were not treated with MG 132 (with the exception of the V2R and IgG1). The complete set of proteins identified in the absence and presence of MG 132 is available in the Supplemental Data section (supp. Table 1 & 2).

Fig. 1

A



B

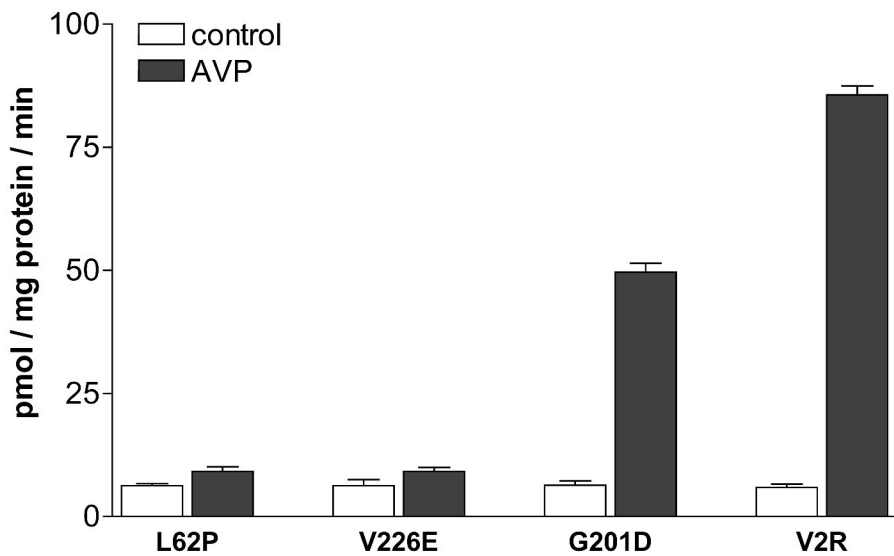


Fig. 2

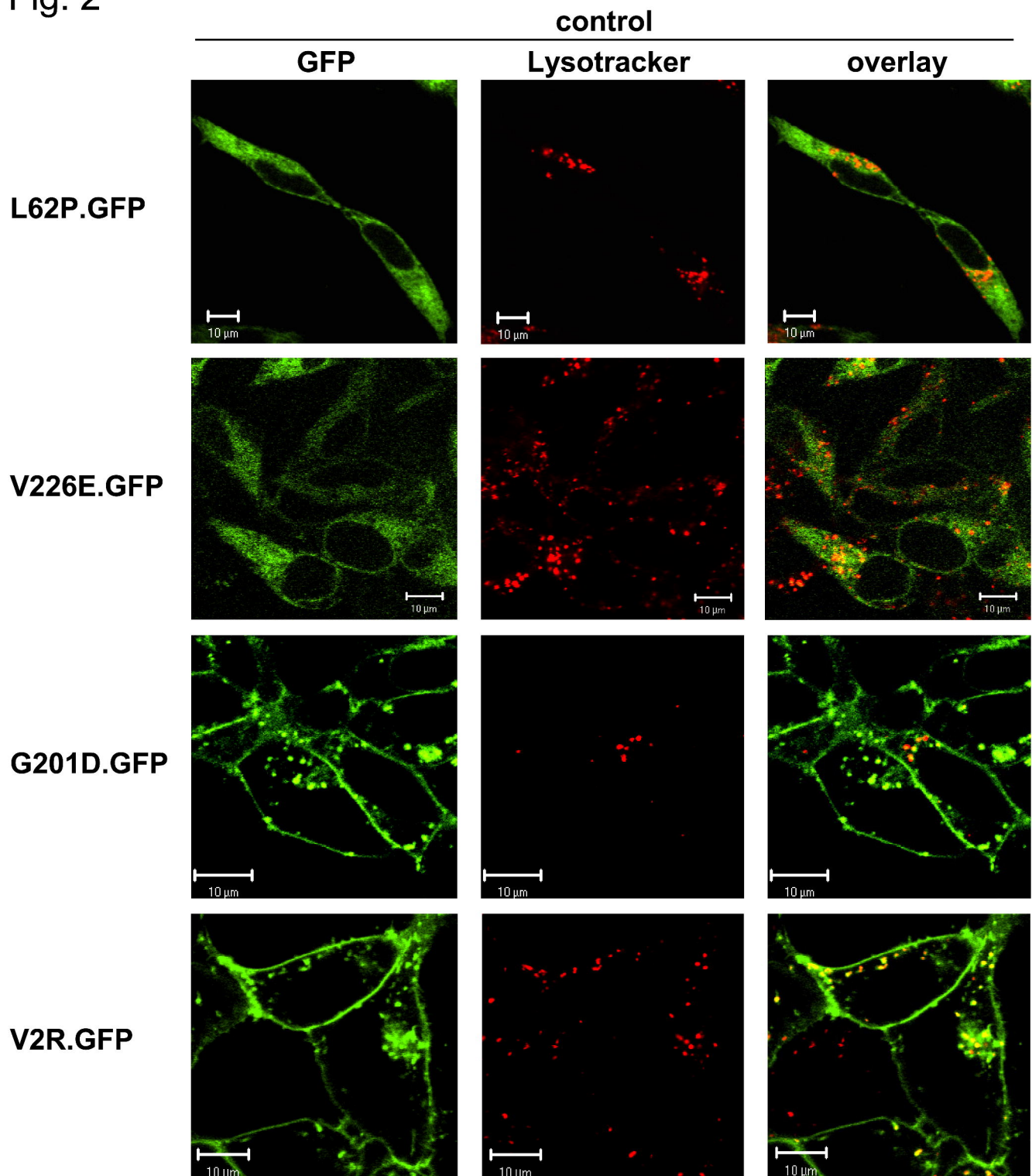


Fig. 3

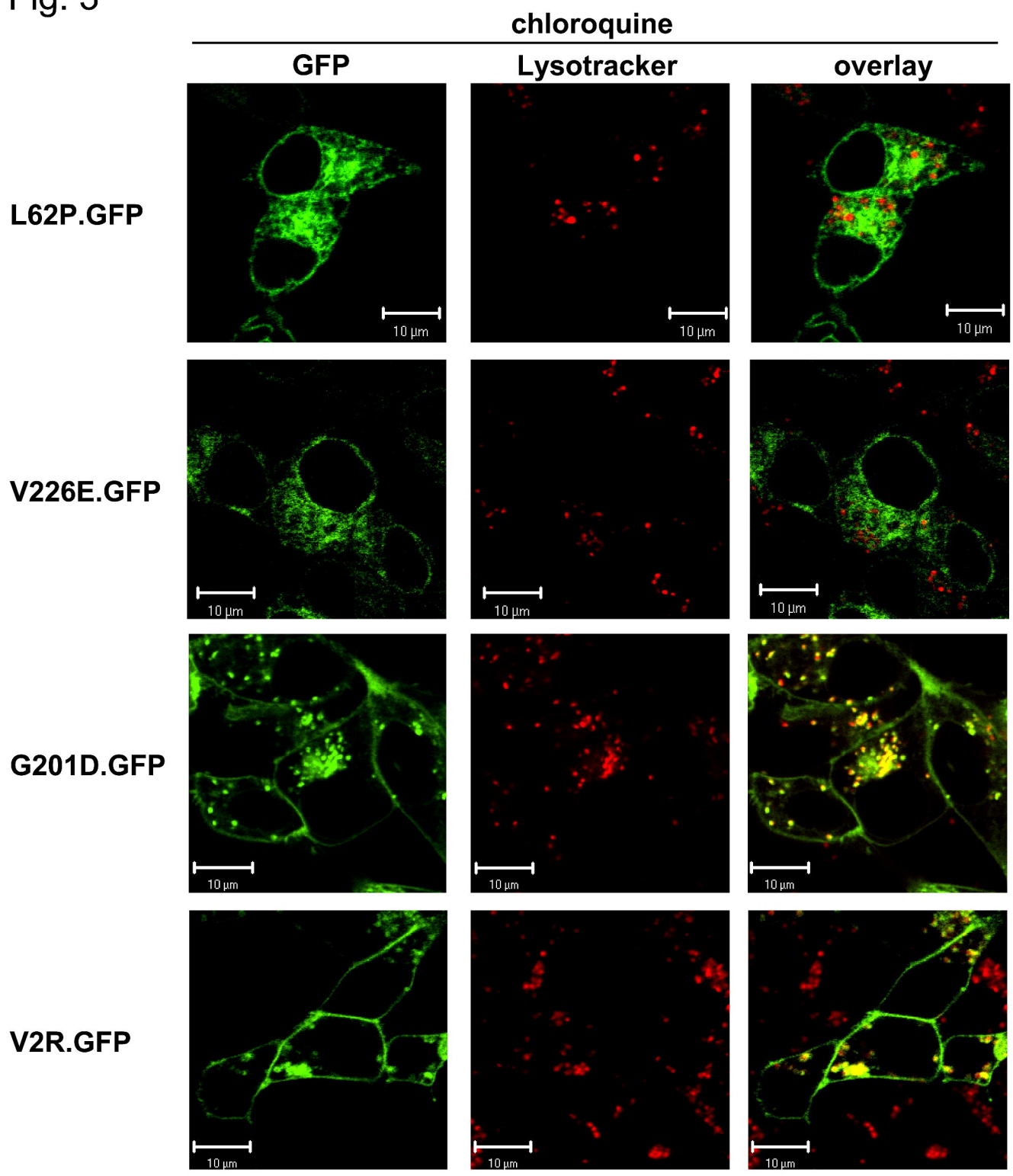


Fig. 4

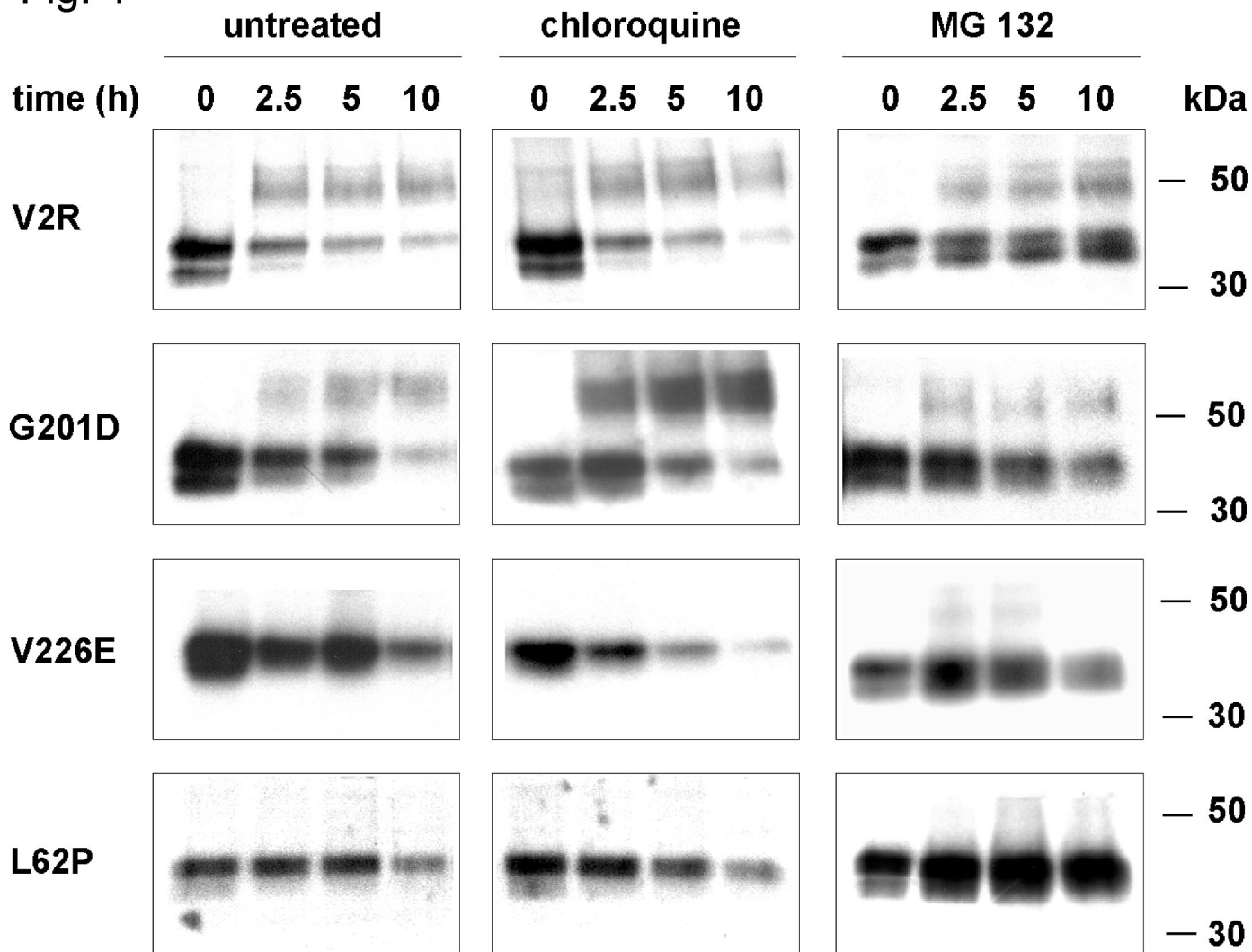
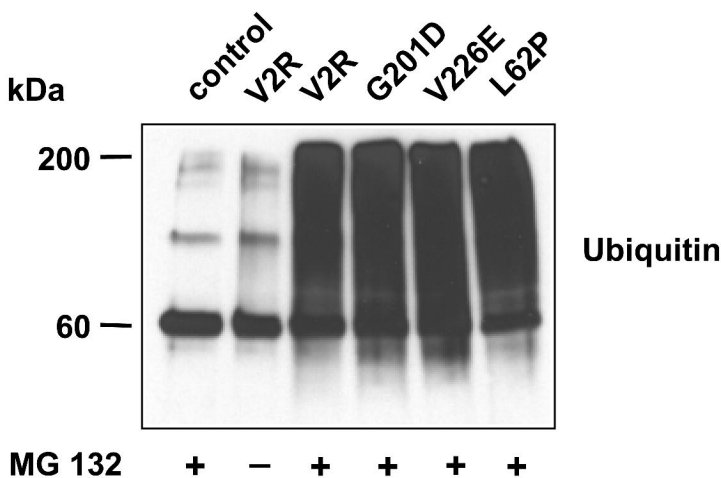


Fig. 5

A



B

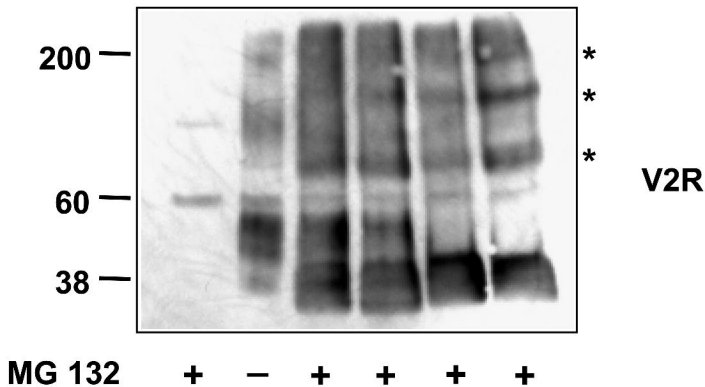
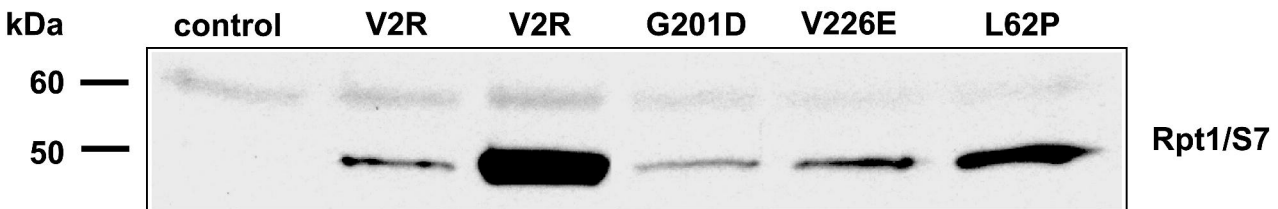
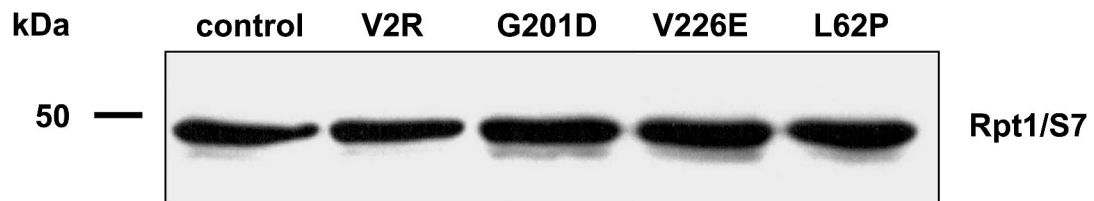
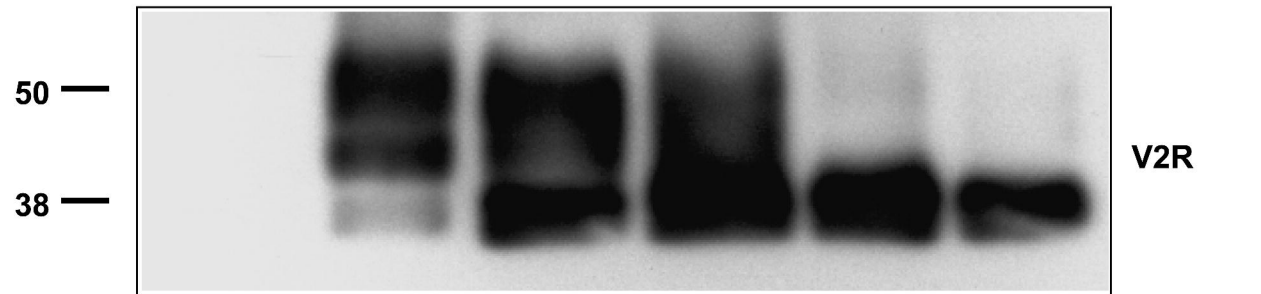
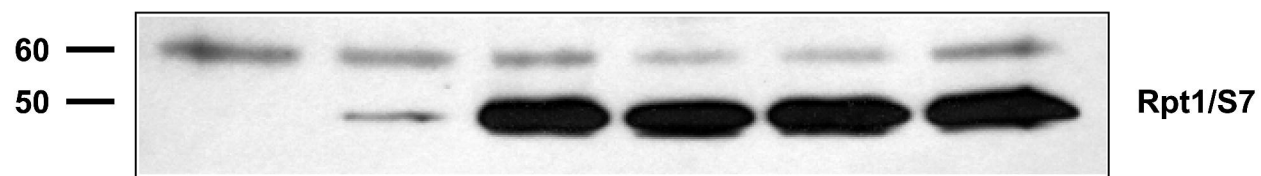


Fig. 6



MG 132 - - + - - -



MG 132 + - + + + +

Fig. 7

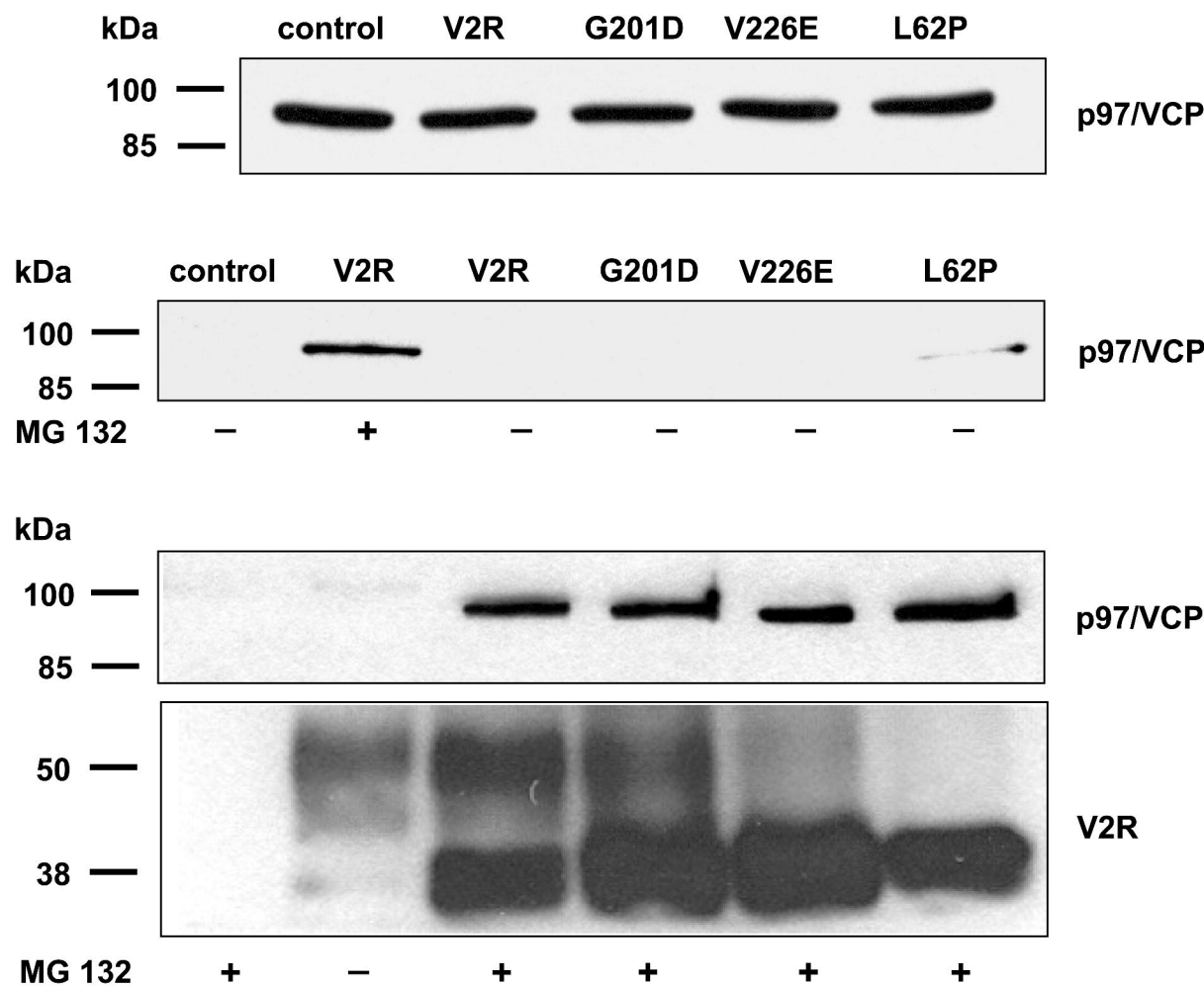
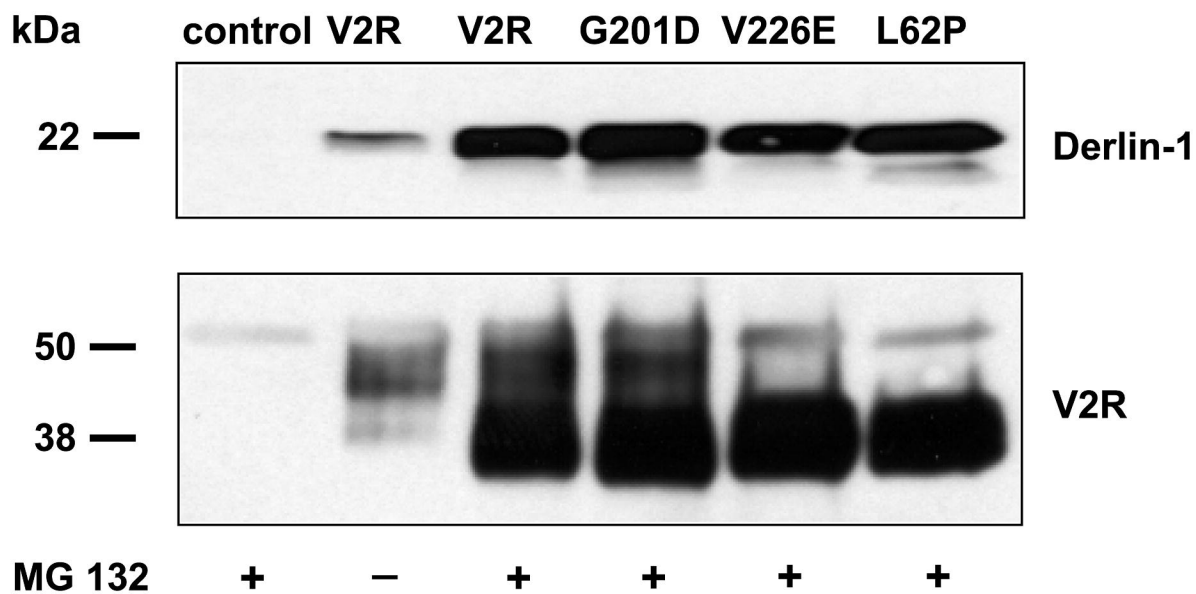
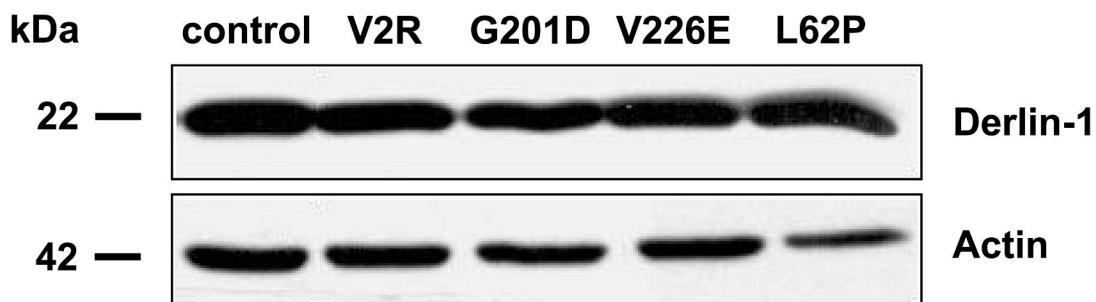


Fig. 8

A



B

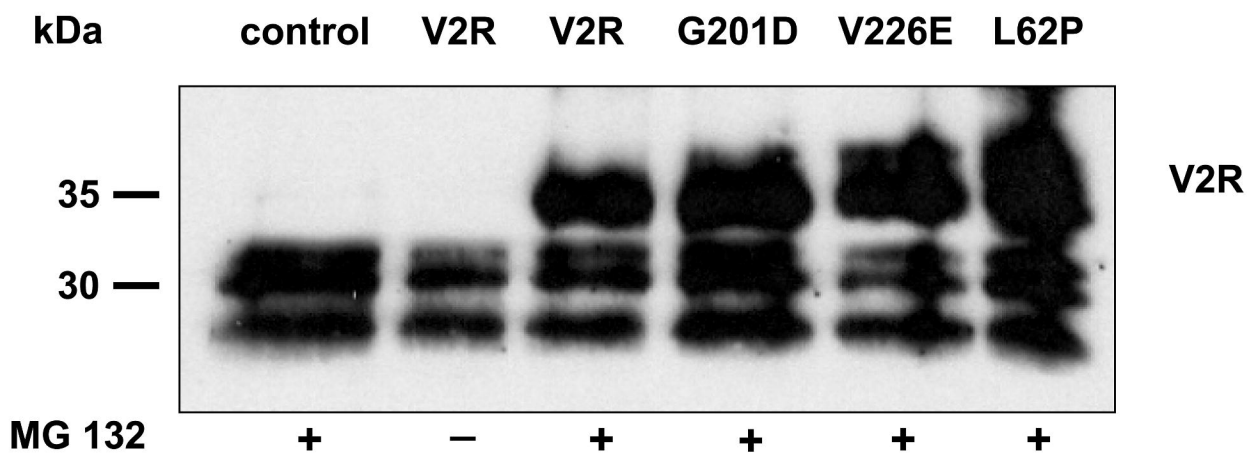


Fig. 9

